Journal of Geophysical Research: Oceans

RESEARCH ARTICLE
10.1029/2018JC014179

Special Section:
The U.S IOOS Coastal and Ocean Modeling Testbed 2013-2017

A Diel Method of Estimating Gross Primary Production: 2. Application to 7 Years of Near-Surface Dissolved Oxygen Data in Chesapeake Bay

Malcolm E. Scully[1]

[1]Applied Ocean Physics and Engineering, Woods Hole Oceanographic Institution, Woods Hole, MA, USA

This article is a companion to Scully et al. (2018), https://doi.org/10.1002/2018JC014178.

Key Points:
- Application of a diel method for estimating gross primary production is applied to 7 years of observing system data from Chesapeake Bay
- The method demonstrates spatial variability with light limitation in the upper Bay transitioning to nutrient limitation in the lower Bay
- Seasonal variability consistent with temperature-dependent growth and interannual variability driven by inorganic nutrient inputs is shown

Correspondence to:
M. E. Scully,
mscully@whoi.edu

Citation:
Scully, M. E. (2018). A diel method of estimating gross primary production: 2. Application to 7 years of near-surface dissolved oxygen data in Chesapeake Bay. *Journal of Geophysical Research: Oceans*, *123*, 8430–8443. https://doi.org/10.1029/2018JC014179

Received 15 MAY 2018
Accepted 26 SEP 2018
Accepted article online 24 OCT 2018
Published online 25 NOV 2018

Abstract A diel method for estimating gross primary production (GPP) is applied to nearly continuous measurements of near-surface dissolved oxygen collected at seven locations throughout the main stem of Chesapeake Bay. The data were collected through the Chesapeake Bay Interpretive Buoy System and span the period 2010–2016. At all locations, GPP exhibits pronounced seasonal variability consistent temperature-dependent phytoplankton growth. At the Susquehanna Buoy, which is located within the estuarine turbidity maximum, rates of GPP are negatively correlated with uncalibrated turbidity data consistent with light limitation at this location. The highest rates of GPP are located immediately down Bay from the estuarine turbidity maximum and decrease moving seaward consistent with nutrient limitation. Rates of GPP at the mouth (First Landing Buoy) are roughly a factor of 3 lower than the rates in the upper Bay (Patapsco). At interannual time scales, the summer (June–July) rate of GPP averaged over all stations is positively correlated ($r^2 = 0.62$) with the March Susquehanna River discharge and a multiple regression model that includes spring river discharge, and summer water temperature can explain most ($r^2 = 0.88$) of the interannual variance in the observed rate of GPP. The correlation with river discharge is consistent with an increase in productivity fueled by increased nutrient loading. More generally, the spatial and temporal patterns inferred using this method are consistent with our current understanding of primary production in the Bay, demonstrating the potential this method has for making highly resolved measurements in less well studied estuarine systems.

Plain Language Summary A new method for estimating gross primary production from in situ dissolved oxygen data is applied to 7 years of data from Chesapeake Bay. Application of the method highlights pronounced spatial and temporal variability consistent with previous studies employing more labor intensive methods. The method shows significant promise for making high-quality measurements of productivity with high temporal resolution in estuarine systems.

1. Introduction

The complex response of an estuarine ecosystem to eutrophication is governed by a wide range of physical and biogeochemical processes (e.g., Cloern, 2001). The scientific and regulatory communities increasingly rely on numerical models to study and understand these complex interactions, and methods to rigorously evaluate the accuracy of these models are needed. Given the difficulty in making direct measurements of biological rates, model skill often is assessed through comparisons with more easily measured parameters such as dissolved oxygen. However, dissolved oxygen is strongly modulated by both physical and biological processes. In Chesapeake Bay Scully (2013, 2016) demonstrated that a model with no biological variability can simulate dissolved oxygen with high skill (Irby et al., 2016). High skill in simulating dissolved oxygen could lead to the false conclusion that a model accurately represents the underlying biological processes. Comparing biogeochemical models to observed biological rates such as primary production is a more rigorous validation of these models.

In Chesapeake Bay the basic processes that control primary production are relatively well understood. It is generally accepted that primary production is maximal during the summer months (Boynton et al., 1982; Flemer, 1970) even though phytoplankton biomass is maximal in the spring (Malone et al., 1988). The size and intensity of the spring bloom are largely controlled by inorganic nutrient inputs from the Susquehanna River (Fisher et al., 1988, 1992; Harding, 1994; Harding et al., 1986; Malone et al., 1988). The breakdown of algal biomass from the spring bloom regenerates nutrients that can sustain high primary

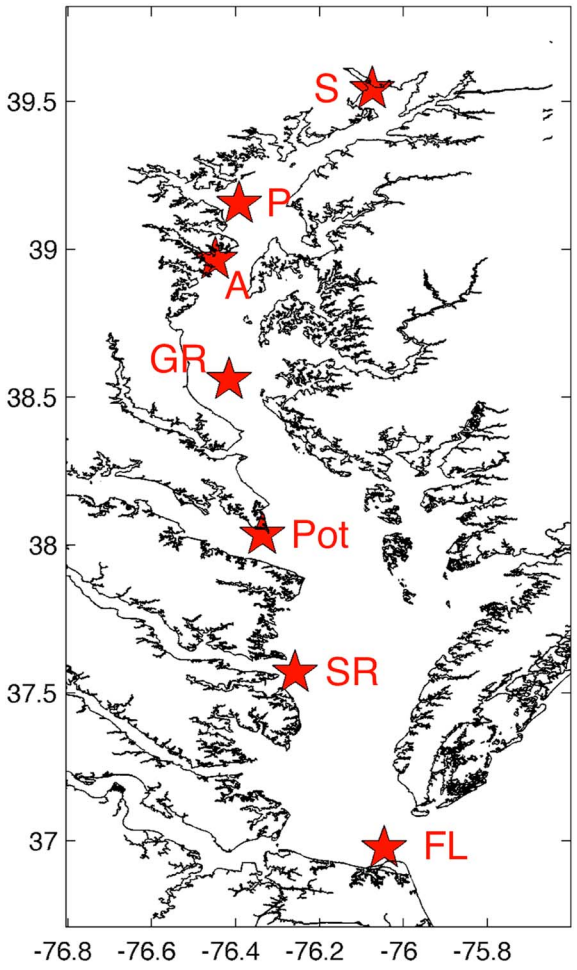

Figure 1. Map of Chesapeake Bay, showing the location of the CBIBS buoys, including Susquehanna (S), Patapsco (P), Annapolis (A), Goose's Reef (GR), Potomac (Pot), Stingray Point (SR) and First Landing (FL).

productivity throughout the summer months (Boynton & Kemp, 1985). The out-of-phase relationship between primary production and chlorophyll often is attributed to high rates of zooplankton grazing during the summer months (Malone, 1992).

In addition to this well-established temporal variability in productivity, Chesapeake Bay experiences pronounced spatial variability as well. Primary production transitions from primarily light limited in the upper Bay to nutrient limited in the lower Bay (Fisher et al., 1988; Harding et al., 1986). Chesapeake Bay has a well-defined estuarine turbidity maximum (ETM) that is typically located near the limit of salt (Sanford et al., 2001; Schubel, 1968). The presence of the ETM and the associated light limitation inhibits primary production in this region, despite the high loads of dissolved inorganic nutrients delivered by the Susquehanna River. The maximum in both primary production and phytoplankton biomass typically is found downstream from the ETM, and decreasing levels of nutrients reduce primary productivity in the lower estuary (e.g., Harding et al., 1986).

This basic conceptual model for the spatial and temporal variations in productivity in Chesapeake Bay has emerged from decades of research. Much of this understanding was derived from rates measured using traditional bottle incubation techniques. Bottle incubations cannot provide temporal resolution at most locations without a significant effort to reoccupy a given location with a ship. There are a few notable exceptions where long-term measurements of primary production that resolve both seasonal and interannual variability have been made (Gallegos, 2012, 2014; Gallegos & Neale, 2015), but these data sets are rare.

Measuring rates of primary production from in situ instrumentation represents a potentially powerful alternative to measuring rates from bottle incubations. Methods that quantify primary production by measuring diel changes in oxygen concentration have a long history of use in aquatic ecosystems (e.g., Odum, 1956). A primary obstacle to the successful use of these methods in estuaries is the contribution that physical processes (vertical mixing and horizontal advection) have on changes in oxygen concentration (Boynton & Kemp, 1985; Howarth et al., 1992; Swaney et al., 1999). Thus, even though we are collecting data with unprecedented spatial and temporal resolution due to advancements in instrument technology and the proliferation of observing systems, our ability to measure basic biological rates has not kept pace.

In this paper, a proposed diel method for estimating gross primary production (GPP; Scully, 2018) is applied to 7 years of observing data collected through the Chesapeake Bay Interpretive Buoy System (CBIBS). Data from seven stations spanning the full estuarine gradient are analyzed providing information about spatial variations in GPP and temporal variations at a variety of time scales. While a companion paper (Scully, 2018) focuses on evaluating the accuracy of the method by applying it to numerical model output, the goal of this paper is to compare the insight gained from the application of the method to field data to the well-established conceptual model of productivity in Chesapeake Bay. While this is not a validation of the method, it demonstrates the potential of the method for providing fundamental insights into the underlying biological processes.

2. Methods

2.1. Data

The CBIBS program maintains 10 buoys throughout the Chesapeake Bay. This paper analyzes data collected between 1 January 2010 and 31 December 2016 at seven locations along the main stem of the Bay: Susquehanna, Patapsco, Annapolis, Goose's Reef, Potomac, Stingray Point, and First Landing (Figure 1). The

Susquehanna Buoy is not deployed during the winter months to avoid damage by ice, but with a few exceptions, nearly continuous data are available at all the other locations. Each buoy makes hourly observations of temperature, salinity, dissolved oxygen, chlorophyll fluorescence, and turbidity with a WETLabs WQM, equipped with an antibiofouling injection system and optical wipers. The WQM is located in the buoy well ~0.5 m below the water surface. All of the data used here are available for download through the CBIBS website (http://buoybay.noaa.gov). The dissolved oxygen data do not have any obvious data quality issues, and the hourly data downloaded from the CBIBS website are used. The quality of the chlorophyll and turbidity data is harder to assess, and there are periods when obvious sensor fouling results in inaccurate data. While these data are not essential to the analysis below, they are used for both qualitative interpretation and quantitative estimates for comparison with previous studies. In an attempt to remove any spurious data very simple criteria are used; any chlorophyll data below a reported value of 1 μg/L and any turbidity data greater than 35 NTU are excluded from the analysis.

Measurements of solar irradiance are not collected at the CBIBS buoys. Instead, the downward shortwave radiation flux from the National Centers for Environmental Prediction North American Regional Reanalysis (NARR) model (https://www.esrl.noaa.gov/psd) is used to provide an estimate of incoming radiation. The NARR model has 32-km spatial resolution and provides output every 3 hr. For this analysis, the model output is linearly interpolated in space to best match the locations of the CBIBS buoys and interpolated in time to provide hourly estimates of irradiance to match the frequency of the CBIBS data. While in situ estimates of light attenuation are not made at the CBIBS buoys, estimates of the large-scale diffuse light attenuation coefficient at 490 nm (Kd-490) are available from Moderate Resolution Imaging Spectroradiometer (MODIS) satellite data (ftp://ftp.star.nesdis.noaa.gov/pub/socd1/ecn/data/modis/k490noaa/monthly/cd/; Wang et al., 2009). These estimates have a spatial resolution ~1 km and a temporal resolution of ~30 days. The Kd-490 data are used in an attempt to provide quantitative estimates of in situ light. As with the NARR data, the satellite estimates of Kd-490 are interpolated in both time and space to match the CBIBS data.

2.2. Analysis

A detailed description of the diel method is provided in a companion paper (Scully, 2018). However, for clarity the basic method is repeated here in abbreviated form. The method is based upon the conservation equation for oxygen

$$\frac{\partial O_2}{\partial t} = GPP - CR - u_i \nabla O_2 + \frac{\partial}{\partial z} K_z \frac{\partial O_2}{\partial z} \tag{1}$$

where the time rate of change of oxygen (first term on left-hand side) is driven by biological production by GPP and consumption by community respiration (CR). Advection (third term on right-hand side) and the divergence in vertical turbulent flux (fourth term) are the physical processes that contribute to temporal variations in oxygen. Here the vertical flux is represented as the product of an eddy viscosity (K_z) and the vertical gradient in oxygen. At the surface ($z = 0$), the flux (F_{surf}) is equal to the air-sea gas exchange, but it is the divergence in this flux that directly contributes to variations in oxygen. As discussed in Scully (2018), only in an integrated sense and for conditions where there are no vertical gradients in oxygen within the surface mixed layer can the divergence in vertical flux at any discrete point be estimated using bulk parameterization (e.g., F_{surf}/z_{mix}).

The method relies on a simplified representation of equation (1) expressed as

$$\frac{\partial O_2}{\partial t} = P_m \tanh\left(\frac{\alpha E}{P_m}\right) + \Delta O_2 \tag{2}$$

where the first term on the right-hand side of (2) represents GPP and ΔO_2 represents the sum of all the remaining terms including the contributions of advection, the vertical divergence in turbulent oxygen flux, and CR. The method assumes that ΔO_2 can be estimated simply as the observed time rate of change of oxygen during the nighttime hours. The estimate of ΔO_2 does not distinguish between the contributions of physical processes and CR, so the method can only directly estimate GPP. After removing ΔO_2, a two-parameter least squares regression between the observed time rate of change of oxygen and incoming solar radiation is performed to provide estimates of the maximum photosynthetic rate (P_m) and the slope (α) of the light-limited portion of the photosynthesis-irradiance (PE) curve. The ratio P_m/α sets the saturating

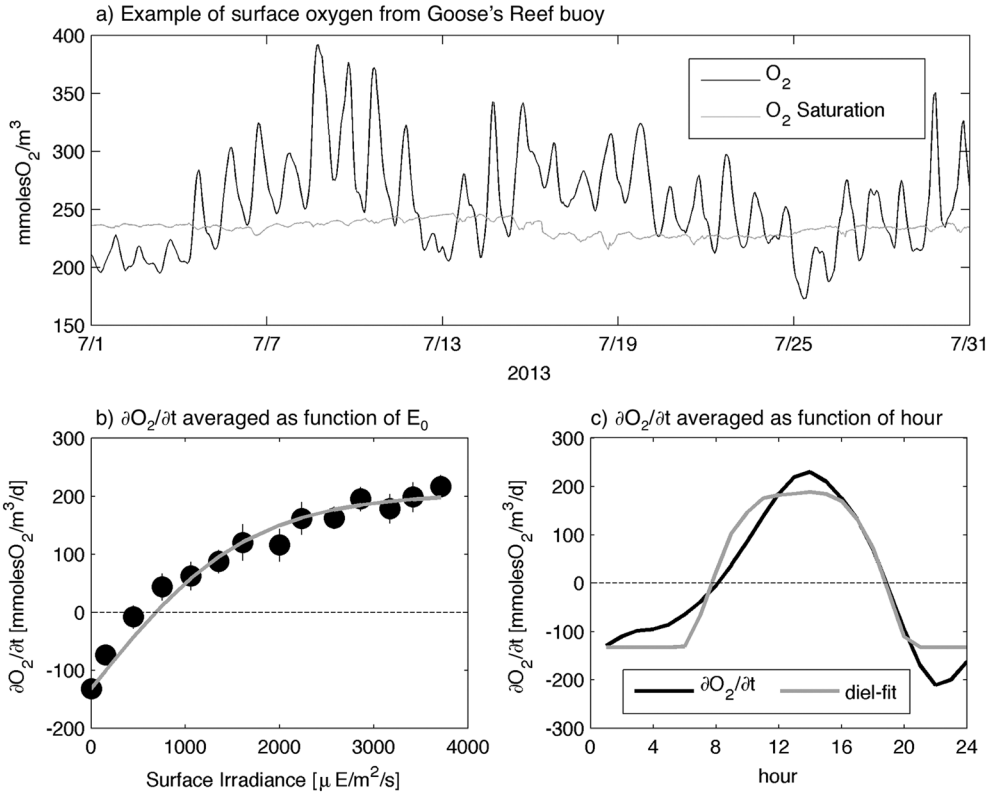

Figure 2. (a) Example of near-surface dissolved oxygen data (back line) from the Goose's Reef buoy from July 2013 compared to saturation value (gray line) based on the observe temperature and salinity. (b) The observed time rate of change of the oxygen date in (a) bin averaged as a function of the surface irradiance. (c) The observe timed rate of change of the data in (a) bin averaged as a function of the hour of the day (black line) to highlight the diurnal variability compared to the estimated primary production (GPP + CR) from the fit shown in (b). The vertical lines in (b) represent 95% the confidence interval, and the gray line is the inferred PE curve from the best fit to the data. GPP = gross primary production; CR = community respiration; PE = photosynthesis-irradiance.

irradiance (E_k) where phytoplankton growth transitions from light-limited ($E < E_k$) to light-saturated growth. In order to avoid aliasing by horizontal currents driven by tidal advection, Scully (2018) recommends applying the method to 15 days of data. This not only minimizes the correlation between semidiurnal and diurnal processes but also provides a sufficient time window to statistically related diurnal changes in oxygen to diurnal variations in light. In this analysis the estimate of ΔO_2 is made by averaging $\partial O_2/\partial t$ for all conditions when light is zero over a 15 day period, denoted $\Delta\widehat{O}_2$, where the hat indicates that the value is obtained when $E = 0$.

To quantify spatial and low-frequency (monthly) variations in light availability, the vertical profile of light is estimated as

$$E = 0.43\, E_0 \exp[K_d z] \tag{3}$$

where E_0 is the downwelling shortwave radiation from the NARR model, K_d, is the attenuation coefficient for light estimated using the Kd-490 value of from the MODIS satellite data and 0.43 is the fraction of the downward shortwave radiation that is available for photosynthesis (Fennel et al., 2006). Estimates of the PE curve parameters are typically normalized by the chlorophyll-*a* concentration, which is denoted with a superscript *B* (P_m^B and α^B).

3. Results

3.1. Example of the Method

To illustrate the application of the method, data from the Goose's Reef buoy collected during July 2013 are presented in Figure 2a. During this period the observed dissolved oxygen concentration exhibits

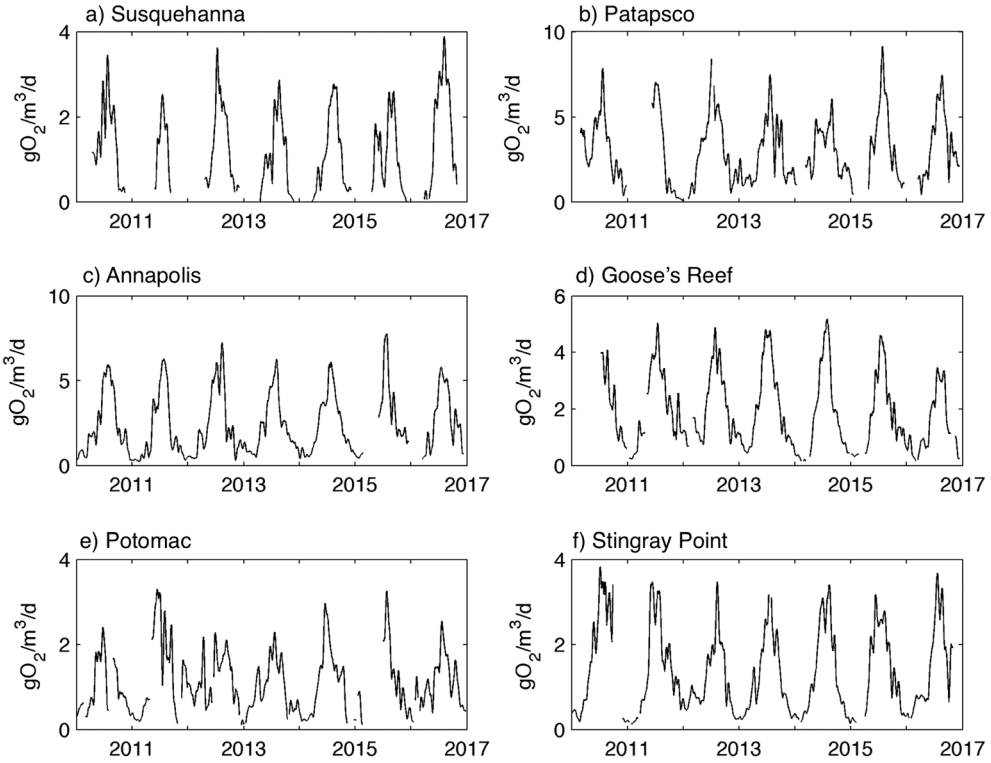

Figure 3. Estimates of the volumetric rate of community respiration from application of the diel method to surface oxygen data at six of the Chesapeake Bay Interpretive Buoy System buoy locations. Estimates of the photosynthesis-irradiance curve parameters (P_m and α) have 15-day temporal resolution and are applied to the hourly surface irradiance data. The resulting time series is smoothed with a 25-day boxcar filter to remove higher-frequency variability. Gaps in each plot represent periods of no data or negative values of community respiration. Data from First Landing are not shown.

pronounced diurnal variability ranging from roughly 100% saturation during the early morning hours to values in excess of 160% saturation during late afternoon. The time rate of change of oxygen during this period displays a functional form consistent with the assumed model (Figure 2b) including the basic diurnal variability (Figure 2c).

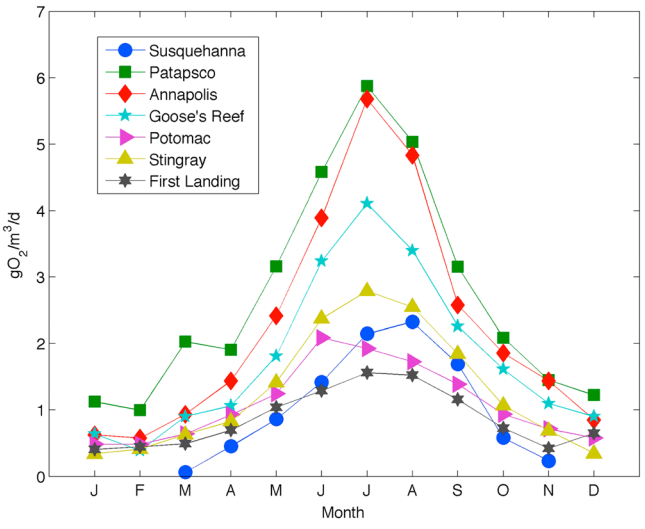

Figure 4. Monthly averaged values of gross primary production averaged over 7 years at all seven Chesapeake Bay Interpretive Buoy System buoy locations including Susquehanna (blue circles), Patapsco (green squares), Annapolis (red diamonds), Goose's Reef (cyan pentagons), Potomac (purple arrows), Stingray Points (gold triangles), and First Landing (black hexagons).

3.2. Seasonal Variability

Even though the parameters of the PE curve are only estimated with 15-day resolution, applying the estimates of the PE curve to the hourly surface irradiance from the NARR model provides estimates of GPP with higher-frequency variability. However, since variations in P_m and α with frequencies higher than 15 days are not resolved, the hourly estimates of GPP are averaged with a 15-day boxcar filter providing estimates of GPP at the seven CBIBS buoys for the period 2010–2016 (Figure 3). At all locations there is clear seasonal variability with rates of GPP increasing throughout the spring, reaching maximum values in middle July before decreasing during late summer and into the fall (Figure 4). At seasonal time scales, estimates of GPP vary by more than a factor of 30 at all locations consistent with temperature-dependent phytoplankton growth. To illustrate this temperature dependence, the data at each station are bin averaged as a function of temperature (Figure 5). These bin-averaged data are fit with a least squares regression after log transforming the rates of GPP. This log linear regression is used to calculate the Q_{10} value for each station. The estimates of Q_{10} range from 1.78 to 3.55. The highest Q_{10} value

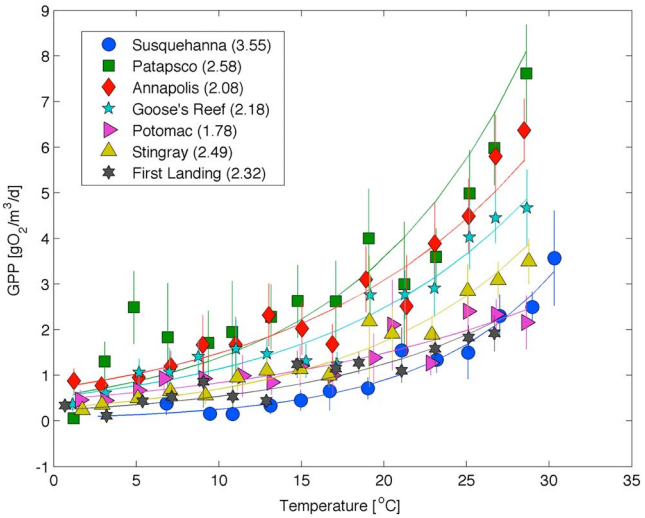

Figure 5. Values of GPP, averaged as a function of water temperature, at all seven CBIBS buoy locations. The symbols are the same as in Figure 4, and the vertical lines represent the 95% confidence interval. The solid lines are the best fit log linear regression, and the values of Q_{10} reported in the legend are based on these fits. GPP = gross primary production; CBIBS = Chesapeake Bay Interpretive Buoy System.

of 3.55 was found at the Susquehanna Buoy, and excluding this value reduces the range to 1.78–2.58.

While the seasonal cycle of GPP at all seven locations is consistent with a temperature-dependent physiological process, there are some notable deviations. At the Susquehanna buoy GPP is reduced during early spring and peaks somewhat later than temperature. As a result, the estimated productivity at the Susquehanna buoy is much lower than all the other locations in early spring but exceeds the estimated values at the two southernmost buoys later in the summer (Figure 4). This is most likely due to the seasonal progression of light limitation at the Susquehanna location (see below). High river discharge and the associated sediment loading in the spring give way to lower sediment concentrations in the summer, when water temperature increases. The increase in GPP from spring to summer is enhanced by greater water clarity and less light limitation as water temperatures rise. As a result, the higher Q_{10} value at the Susquehanna buoy most likely is the result of the correlation between water temperature and light availability at this location and not a true physiological temperature response. In contrast, at all of the other locations GPP peaks earlier than temperature. At these locations GPP is shifted relative to temperature so that GPP is generally higher than the exponential fit during spring and early summer and lower than the exponential fit during late summer and early fall. This deviation from strictly Q_{10} behavior is consistent at all six locations down Bay from the Susquehanna location and could be explained by the seasonal development of nutrient limitation.

Consistent with the Q_{10} variability in GPP, P_m exhibits an exponential relationship with temperature at all locations (Figure 6a). The highest values of P_m are found at the Patapsco buoy and generally decrease down Bay. Values at the Susquehanna buoy are reduced by ~40% as compared to Patapsco. Estimates of α generally increase with P_m. At seasonal time scales, P_m increases more rapidly than α so that the saturating irradiance (E_k) increases roughly linearly with temperature (Figure 6b). This results in a seasonal pattern with the largest values of E_k occurring during the late summer and early fall. Although temperature and insolation are correlated, temperature generally peaks later in the year than light intensity. The seasonal changes in E_k are more strongly correlated with temperature than insolation, suggesting that this seasonal variability is primarily controlled by temperature and does not reflect light adaptation (Pennock & Sharp, 1986).

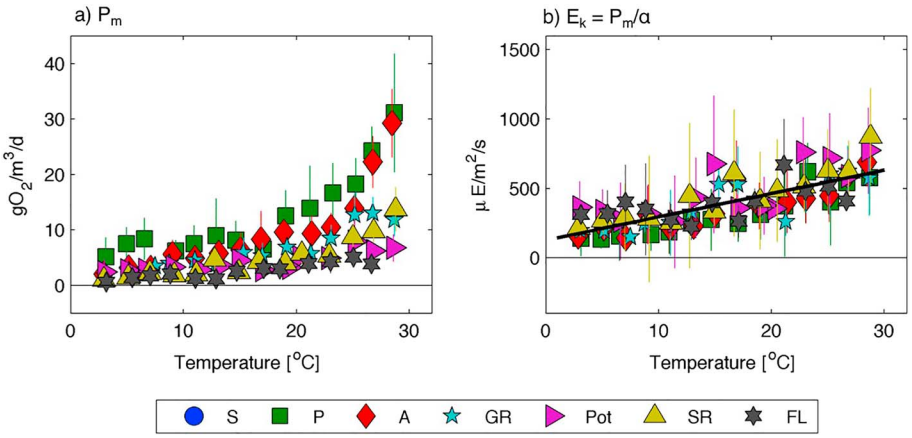

Figure 6. Estimates of the photosynthesis-irradiance curve parameters including (a) the maximum phytoplankton growth are (P_m) and (b) the saturating irradiance ($E_k = P_m/\alpha$), bin averaged as a function of temperature. Symbols are the same as in Figure 4, and the vertical bars represent the 95% confidence interval.

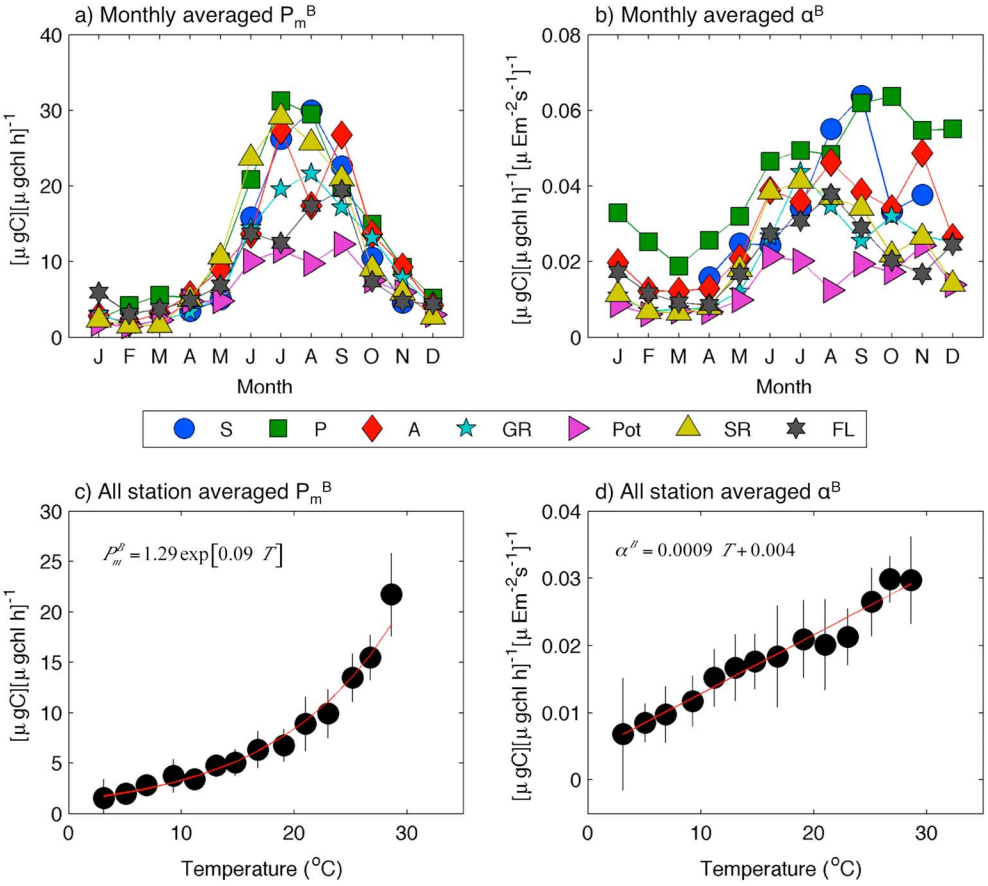

Figure 7. Normalized values of the photosynthesis-irradiance curve parameters including (a) the maximum phytoplankton growth rate (P_m^B) and (b) the initial slope of the photosynthesis-irradiance curve under light-limited conditions (α^B) for each station, bin averaged by month. The different symbols, with represent the individual stations, are the same as in Figure 4. Bay-wide (all seven stations) averages of the same data are represent in (c) and (d), bin averaged as a function of temperature. In (c) and (d), vertical lines represent the 95% confidence interval and curve represented the best fit regression to the data. The data have been converted to carbon-based units using a photosynthetic quotient of 1.4 for comparative purposes.

To facilitate comparison with previous bottle incubation studies, the normalized parameters of the PE curve have been converted to carbon units using a photosynthetic quotient (O_2:C) of 1.4 (Laws, 1991), so that P_m^B has units [μgC] [μgchl h]$^{-1}$ and α^B has units [μgC] [μgchl h]$^{-1}$ [μEm^{-2} s^{-1}]$^{-1}$. At seasonal time scales, P_m^B ranges from 1 to 35 (Figure 7a), with the largest values during summer in the upper and middle Bay. Monthly averaged values of α^B from the proposed diel method range from 0.006 to 0.06 (Figure 7b). While there are differences in the magnitude of P_m^B between the seven stations, a clear logarithmic relationship with temperature is observed at all stations. Aggregating the data from all seven stations yields a single logarithmic relationship with temperature that can reasonably capture most of the data (Figure 7c). Consistent with the nonnormalized values of α, values of α^B vary linearly with temperature and a simple linear regression can reasonably capture this variability when the data from all seven stations are averaged (Figure 7d).

3.3. Spatial Variability

The highest rates of GPP are found at the Patapsco buoy and generally decrease moving down Bay (Figure 8a). The annual mean rate of GPP at the Susquehanna buoy is more than a factor of 2 lower than at Patapsco but somewhat larger than the annual mean rate at First Landing. The general spatial variability in GPP is consistent with the overall spatial variability in chlorophyll concentration, which also is highest at Patapsco and generally decreases moving down Bay (Figure 8b). At seasonal time scales GPP is not

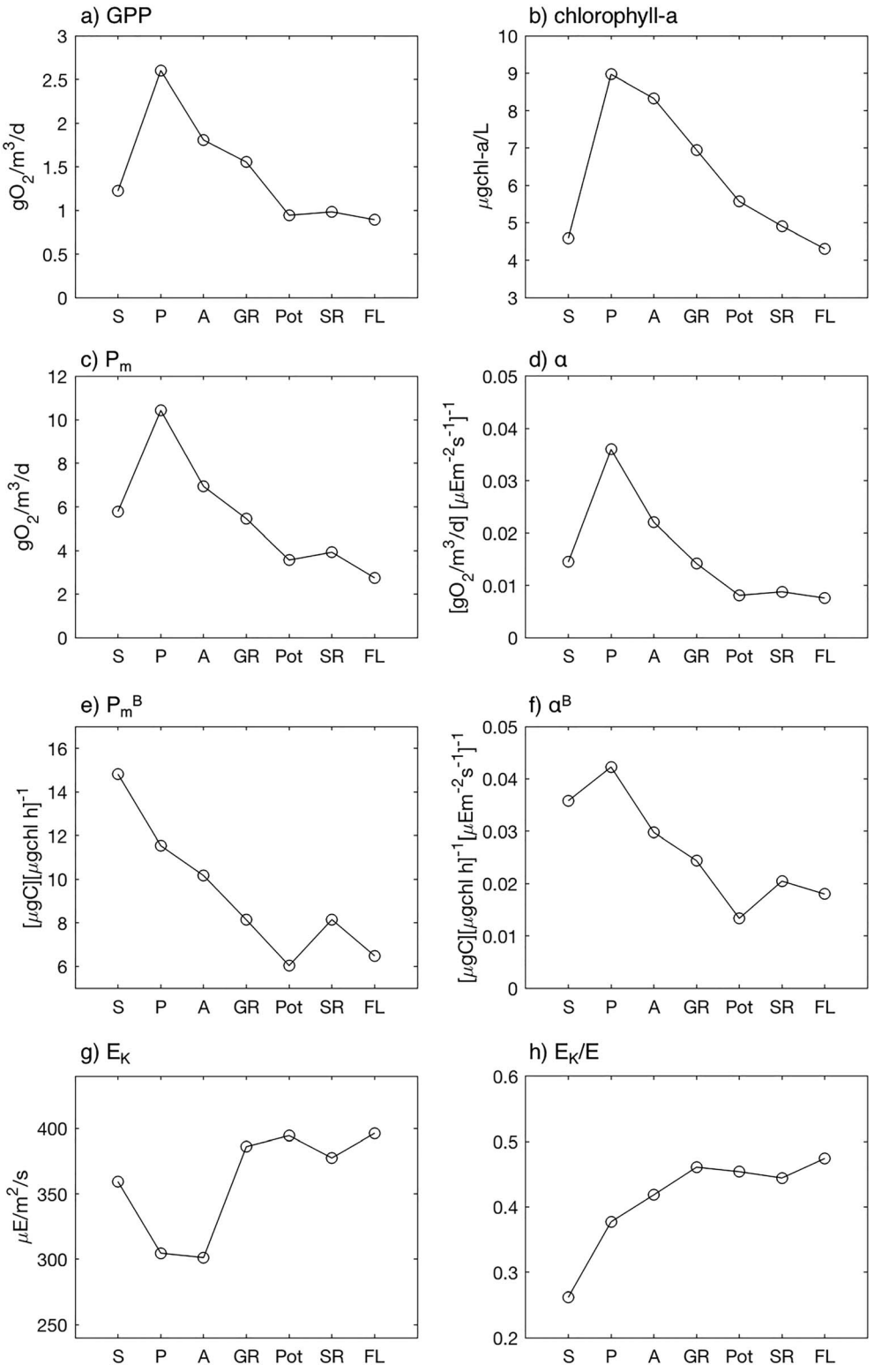

Figure 8. Averaged values of (a) GPP, (b) chlorophyll-*a* concentration, (c) maximum phytoplankton growth rate (P_m), (d) slope of light-limited PE curve (a), (d) normalized phytoplankton growth rate (P_m), (e) normalized slope of light-limited PE curve (a^B), (f) saturating irradiance ($E_k = P_m/a$), and (g) average irradiance normalized by saturating irradiance (E/E_k). Data are plotted as a function of station that are averaged over all available data. Data in (d) and (e) have been converted to carbon-based units using a photosynthetic quotient of 1.4 for comparative purposes. GPP = gross primary production; PE = photosynthesis-irradiance.

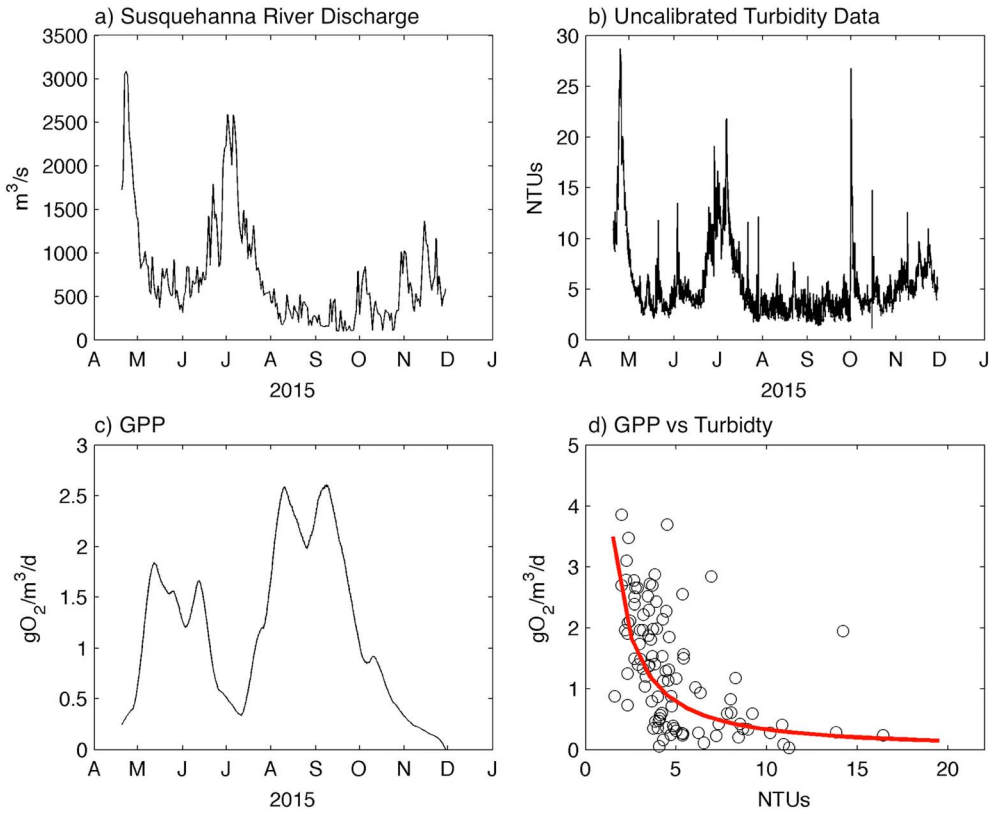

Figure 9. Example of light limitation at the Susquehanna buoy location including (a) Susquehanna River discharge at the USGS Conowingo gauging stations for 2015, (b) uncalibrated turbidity data from Susquehanna buoy for 2015, and (c) estimated GPP for 2015 showing strong negative correlation with water clarity. All (2010–2016) of the estimated of GPP and 15-day average turbidity data from the Susquehanna buoy are plotted in panel (d) highlighting light limitation at this location. USGS = U.S. Geological Survey; GPP = gross primary production.

significantly correlated with chlorophyll measured at the buoys. The along-estuary variability in both P_m and α mirrors that of GPP (Figures 8c and 8d). However, both $P_m{}^B$ and α^B are more spatially uniform and generally decrease moving down Bay (Figures 8e and 8f). Average values of E_k increase somewhat in the down Bay direction, but the spatial trend is not clear and annual average values are all within ~15% of each other (Figure 8g). Using the satellite-derived values of Kd-490 to estimate light availability at $z = -0.5$ m suggests that light limitation (E/E_k) decreases moving down Bay but that all locations are light limited on average (Figure 8f).

The general down Bay decrease in the normalized parameters of the PE curve is consistent with increasing nutrient limitation moving down Bay away from the Susquehanna River. At the Susquehanna buoy the low values of GPP and chlorophyll concentrations appear to be the result of a high degree of light limitation at this location. Figure 9 shows estimates of GPP and the uncalibrated turbidity data for 2015 from the Susquehanna buoy, along with the estimated Susquehanna River discharge from the U.S. Geological Survey Conowingo gauging station. In 2015 the buoy was deployed in late March during high discharge conditions that were associated with high turbidity. Estimates of GPP in the spring are low and only begin to increase in May as the turbidity decreases (Figure 9c). GPP continues to increase during the early summer before decreasing again during a high turbidity event in late June and early July. The midsummer turbidity event coincides with elevated Susquehanna River discharge and estimates of GPP decrease by more than an order of magnitude from middle June to early July. As the turbidity levels decrease in late July, GPP values again increase before decreasing in late fall consistent with the typical season pattern. At the Susquehanna buoy all estimates of GPP (2010–2016) show a negative relationship with the uncalibrated turbidity data ($r = -0.49$; Figure 9d), consistent with light availability controlling GPP at this location.

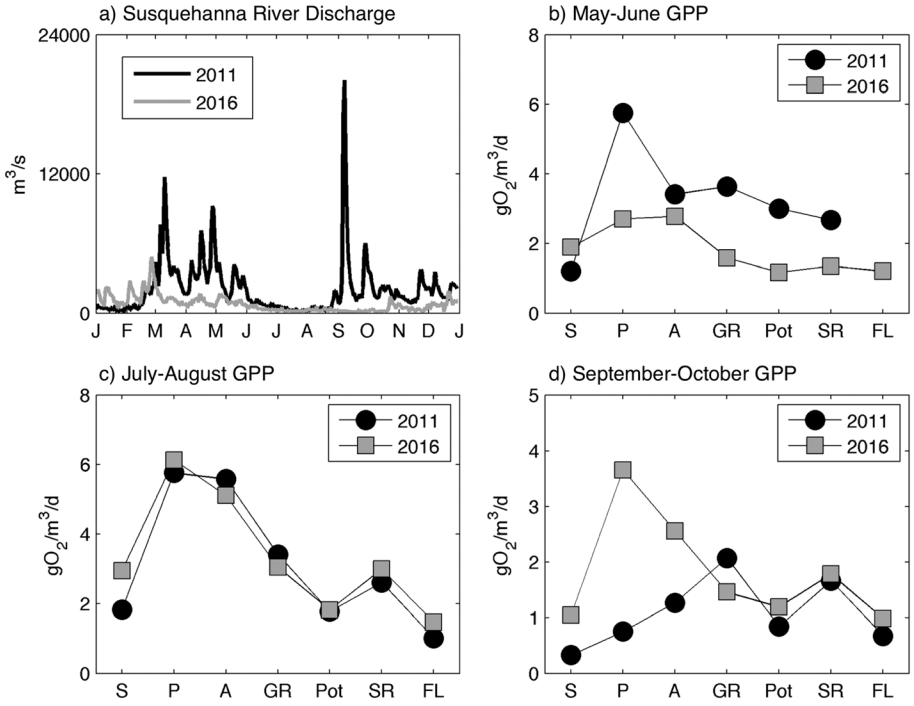

Figure 10. Comparison of GPP estimates for 2011 (black line/circles) and 2016 (gray line/squares) including (a) the Susquehanna River discharge at the USGS Conowingo gauging station and GPP at each station averaged over (b) May–June, (c) July–August, and (d) September–October. Elevated spring river discharge in 2011 increases early summer GPP, but high discharge and sediment loading during tropical storms in fall 2011 suppress GPP in the upper Bay. GPP = gross primary production; USGS = U.S. Geological Survey.

3.4. Interannual Variability

While the seasonal cycle is a robust feature every year, there are significant interannual differences (e.g., Figure 3). To highlight this variability, the estimates of GPP for 2011 and 2016 are compared (Figure 10). For the 7 years of data analyzed here, 2011 had the highest spring river discharge and 2016 had the lowest. In addition, the passage of Hurricane Irene and Tropical Storm Lee resulted in historic inputs of freshwater and sediment to the Bay during the late summer and early fall of 2011 (Palinkas et al., 2014). The high river discharge and associated sediment loading during the spring of 2011 appear to suppress GPP at the Susquehanna location in late spring (Figure 10a). However, estimates of GPP for late spring and early summer in 2011 are elevated at all of the other locations in comparison to 2016. By middle to late summer estimates of GPP for 2011 and 2016 are similar at all locations.

While the high spring river discharge appears to have enhanced early summer GPP at most non-ETM stations, the historic sediment inputs in early fall of 2011 appear to have suppressed GPP in the middle and upper Bay. Estimated rates of GPP for the fall of 2011 are reduced compared to 2016 at the Susquehanna, Patapsco, and Annapolis locations (Figure 10d). Satellite images taken immediately after the passage of Tropical Storm Lee show a sediment plume from the Susquehanna River extending to at least the mouth of the Patuxent River, and sediment cores revealed a distinct flood deposit over the region north the Goose's Reef buoy (Palinkas et al., 2014). The historic sediment inputs associated with this storm appear to have extended the region of light limitation significantly down Bay compared to the traditional location of the ETM.

The control of early summer GPP by nutrient loading from the Susquehanna River is supported by the correlation between interannual variations in Bay-wide rates of GPP for the months June and July with the mean Susquehanna River discharge over the month of March (Figure 11a). A logarithmic relationship based on March river discharge can explain 62% of the variance in the interannual variation in bay-wide GPP averaged over the months June and July. A multiple regression model that includes March Susquehanna River discharge and the mean summer (June–July) water temperature explains 88% of the variance in the observed interannual variability (Figure 11b). In contrast to summer, interannual variations in spring (March–April)

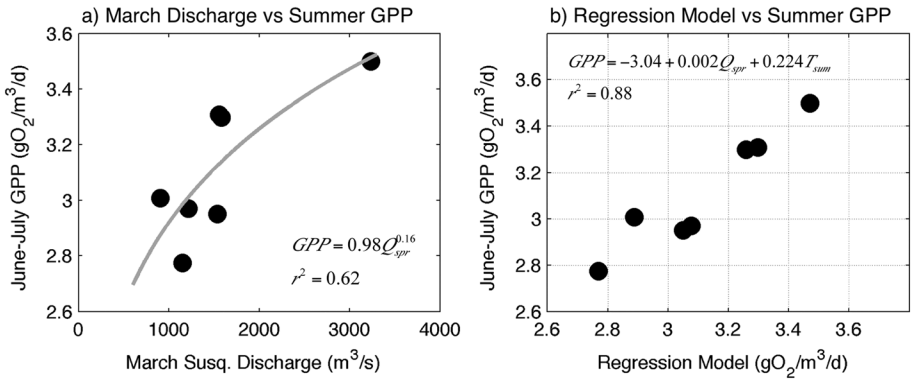

Figure 11. Interannual variability in Bay-wide (all seven stations) GPP averaged over the months of June and July plotted as a function of (a) March Susquehanna River discharge (Q_{spr}) and (b) multiple regression model that includes March Susquehanna River discharge and June–July water (T_{sum}). In (a), the solid line is the best fit log linear regression. GPP = gross primary production.

GPP are negatively correlated with spring Susquehanna River discharge ($r = -0.68$). This presumably reflects light limitation caused by the increased sediment load that accompanies elevated river discharge. The correlation between the uncalibrated turbidity data and GPP in spring is also negative ($r = -0.64$), and a simple multiple regression model that includes spring turbidity data and spring water temperature can explain 83% of the interannual variance in spring GPP. While the statistics of such small data sets must be interpreted with care, the inferred controls on primary production are consistent with previous studies.

4. Discussion

The application of the diel method to 7 years of observations from Chesapeake Bay presented above provides insights that are generally consistent with the basic conceptual understanding of productivity for this well-studied estuarine system. Lomas et al. (2002) found that Q_{10} values for pelagic processes in Chesapeake Bay fell within a range of 1.7–3.4. The estimates of Q_{10} from six of the seven CBIBS locations fall within this range. The approximately linear relationship between α and P_m is consistent with previous data collected in Chesapeake Bay (Harding et al., 1986). Gallegos (2012) reported seasonal variations in monthly averaged values of $P_m{}^B$ of ~1–5 in a shallow subestuary of Chesapeake Bay, with individual estimates as high as ~20. The values of $P_m{}^B$ reported here exhibit the same seasonal pattern reported by Gallegos (2012) but extend to higher overall values. Harding et al. (1986) reported $P_m{}^B$ values of 1.2–15.2 for data collected in the main stem of Chesapeake Bay, so the maximum monthly averaged values of $P_m{}^B$ reported here are roughly a factor of 2 larger than that study. The monthly averaged values of α^B from the proposed diel method range from 0.006 to 0.06 (Figure 7b), which mostly falls within the range of values (0.01–0.132) reported by Harding et al. (1986).

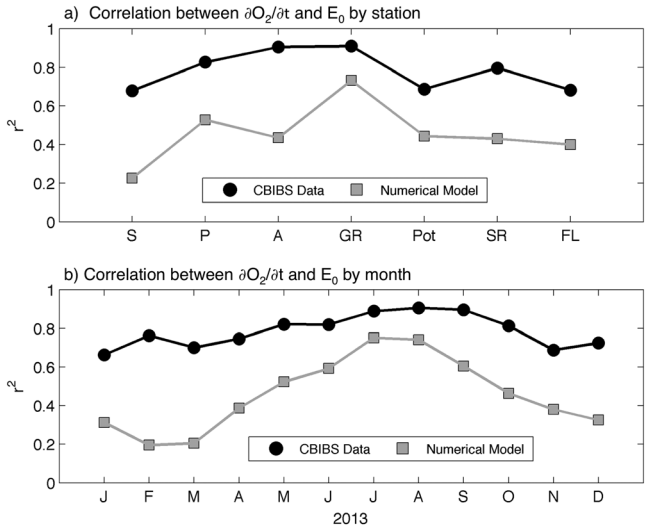

Figure 12. Correlation between incoming solar radiation (E_0) and the time rate of change of dissolved oxygen for 2013, averaged (a) annually at each station and (b) over all stations for each month. The black circles are the CBIBS buoy observation, and the gray squares are the model output of Scully (2018) for the same locations. For this analysis the correlations are calculated after the date and the model output was averaged as function of the day for each month. At all locations and for all months, the observed time rate of change is more highly correlated with the modeled irradiance than the actual model output. CBIBS = Chesapeake Bay Interpretive Buoy System.

Even though the estimates presented in this paper are generally consistent with previous studies employing more traditional methodology, there are notable differences. These differences could result from potential biases associated with the method as outlined in Scully (2018). One source of bias is the contribution of the divergence in vertical oxygen flux to diurnal variations in oxygen. The sign of this bias is a function of vertical position, with underestimated rates of GPP found near the surface and overestimates found near the base on the surface mixed layer. The reported depth of the measurements collected at the CBIBS buoys is

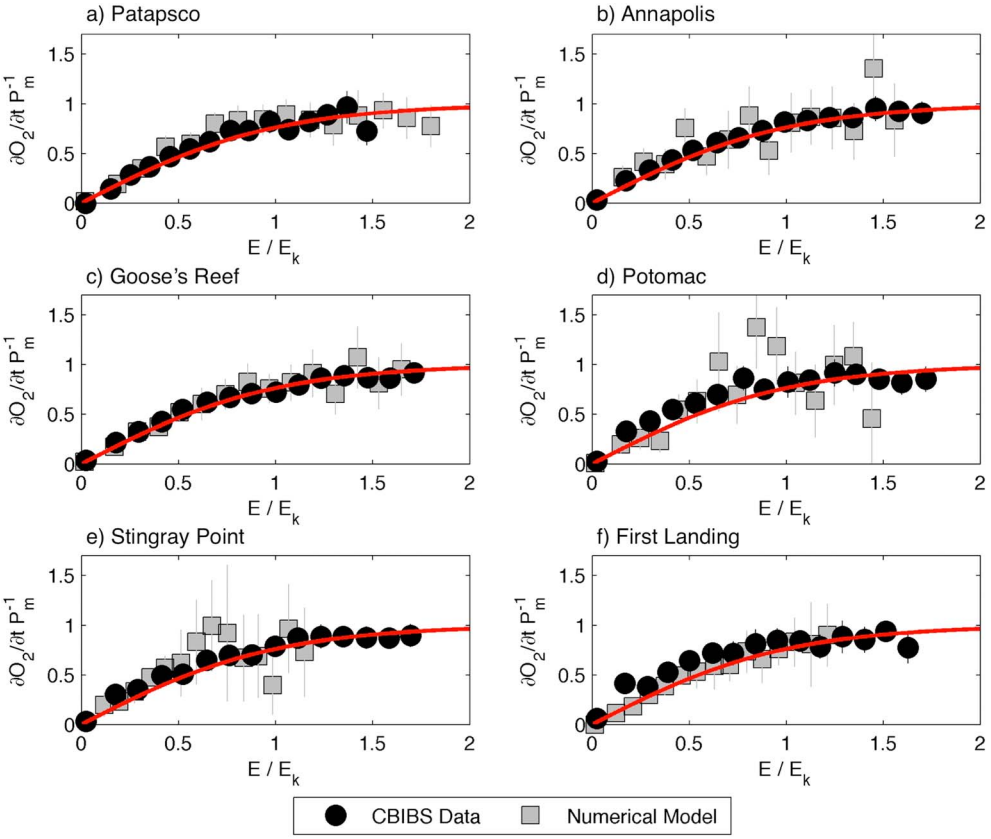

Figure 13. Time rate of change of dissolved oxygen normalized by the estimated maximum phytoplankton growth rate (P_m) plotted as a function of light availability normalized by the estimated saturating irradiance ($E_k = P_m/a$) for (a) Patapsco, (b) Annapolis, (c) Goose's Reef, (d) Potomac, (e) Stingray point, and (f) First Landing. The black circles are the observations at the CBIBS buoys, and the gray squares are the numerical model output of Scully (2018) for the same locations. Only data from 2013 are used, and values are bin averaged as a function of E/E_k. Vertical lines represent the 95% confidence interval, and continuous line is the assumed PE curve. The field data are generally more consistent with the assumed PE curve than the numerical model output. CBIBS = Chesapeake Bay Interpretive Buoy System; PE = photosynthesis-irradiance.

$z = -0.5$ m. Scully (2018) found that data from this vertical position underestimated the actual rate of GPP by up to a factor of 2 for an assumed exponential profile of GPP. For an exponential profile, the vertical location with the least bias is expected to occur roughly at $z = 1.54/K_d$, the depth where the local rate of GPP is equal to the average over the euphotic zone.

Average values of Kd-490 are 2.4 at the Susquehanna buoy and decrease moving down Bay with the four southernmost buoys all falling between 0.8 and 0.9. Based on these averaged values, all the measurements were collected closer to the surface than the location with minimum bias. Data from the upper Bay regions where K_d is higher are closer to this vertical position than those in the lower Bay where K_d is lower, suggesting greater underestimation of GPP in the lower Bay. Therefore, it is possible that some of the down Bay decrease in GPP inferred from the diel method is caused by increasing underprediction of GPP moving down Bay. However, Scully (2018) also suggested that magnitude of the bias was greater in regions where the surface mixed layer depth (z_{mix}) exceeded the photic depth (z_{eu}). In the low-salinity upper Bay region near the Susquehanna buoy the model predicted $z_{mix} > z_{eu}$ and the biases were larger in this region. However, the CBIBS buoys are much closer to the optimal depth (e.g., $z = 1.54/K_d$), so this bias may be less than for the model simulations.

In the data presented above values of $P_m{}^B$ were roughly a factor of 2 larger than the previously published data from Chesapeake Bay. This could simply reflect natural spatial and temporal variability. However, the estimates presented here use a number of highly uncertain parameters including buoy-derived estimates

of chlorophyll-*a* concentration, light availability inferred from an atmospheric model, satellite estimates of K_d, and a fixed photosynthetic quotient. Systematic biases in any of these parameters could explain the higher values of $P_m{}^B$ that are inferred in this paper. The analysis of Scully (2018) suggests that the diel estimates of both P_m and α may be biased low for data collected near the ocean surface. Estimates of α^B are generally consistent with previously published values, but $P_m{}^B$ is generally larger, so this is unlikely the cause of this discrepancy. It is important to note that for the light-limited conditions inferred from this data, estimates of GPP are much more sensitive to the value of α than P_m. Furthermore, estimates of α are likely to be more accurate for light-limited conditions because the light-saturated conditions ($E > E_k$) needed to resolve P_m might not be experienced in situ.

Scully (2018) suggested that errors associated with vertical mixing are enhanced when GPP varies strongly in the vertical and that a more uniform vertical distribution of GPP would reduce errors associated with vertical mixing. There are number of reasons why the natural profile of GPP might be more vertically uniform than the typically assumed exponential profile. Even though the analysis presented above suggests that conditions in Chesapeake Bay are strongly light limited, it is possible that the vertical variation in GPP is more uniform than an exponential profile and that the contributions of vertical mixing in the model of Scully (2018) are too high. Evidence for this comes from a simple analysis where the observed time rate of change of oxygen is correlated with the NARR model of incoming solar radiation. At all seven locations and in every month of the year, the correlation between the observed time rate of change of oxygen and the modeled NARR solar radiation is higher than for the same analysis performed on the model output of Scully (2018) (Figure 12). So even though the numerical model uses the NARR solar radiation to force GPP in the model, the resulting time rate of change of oxygen in the model has a lower correlation with E_0 than the data. A plausible explanation for this is that the contribution of vertical mixing is much greater in the model because of the assumed exponential profile of GPP that is employed.

In addition to decreasing the correlation between the time rate of change of oxygen and the incoming solar radiation, the contribution of advection and mixing also could alter the consistency of the observed $\partial O_2/\partial t$ with the assumed functional form of the PE curve (e.g., equation (2)). At all seven CBIBS locations the observed $\partial O_2/\partial t$ data are highly consistent with the proposed hyperbolic tangent formulation when normalized by the estimated values of P_m and α (Figure 13). An identical analysis performed on the model output of Scully (2018) is less consistent, even though the model uses this exact numerical representation for the PE curve. Deviations from this curve for the numerical model must be caused by advection or mixing suggesting that these physical processes are overestimated in the model as compared to the data. This is not to say that the estimates of GPP presented in this paper are without error, but the magnitude of the errors presented in Scully (2018) may represent an upper bound.

5. Conclusion

In this paper an in situ diel method for estimating GPP is applied to 7 years of surface oxygen data in Chesapeake Bay. Application of the method provides a detailed description of the spatial and temporal variations in GPP. At seasonal time scales inferred rates of GPP vary in a manner consistent with temperature-dependent phytoplankton growth at all stations. Q_{10} values outside of the ETM region fall within a relatively narrow range from 1.78 to 2.58, consistent with previous estimates made in this estuary (Lomas et al., 2002). While the clear seasonal cycle is observed at all locations, there are systematic deviations from purely temperature-dependent process. At the northernmost location within the ETM (Susquehanna), GPP is depressed in spring and elevated in late summer consistent with light limitation driven by the high TSS loads that accompany elevated spring river discharge. At all non-ETM locations the deviations from Q_{10} are opposite with GPP depressed in late summer relative to a purely temperature-dependent rate, consistent with nutrient limitation.

The transition from light-limited conditions in the ETM to nutrient limitation down Bay is well captured in this analysis. Data from the Susquehanna buoy show clear evidence for light limitation at a variety of time scales controlled by sediment input from the Susquehanna River. The highest rates of GPP are located at the northernmost location outside of the ETM (Patapsco) and generally decrease down Bay consistent with increasing nutrient limitation. The importance of inorganic nutrient loading from the Susquehanna River is highlighted by the positive correlation between interannual variability in summer (June–July) GPP and the

March Susquehanna River discharge. This is consistent with the basic understanding of what controls primary production in Chesapeake Bay and provides a direct observational link between measured in situ rates of GPP and inorganic nutrient loads. A multiple regression model that includes spring Susquehanna River discharge and summer water temperature can explain 88% of interannual variance in Bay-wide GPP over the 7 years that are analyzed. The fundamental description of the spatial and temporal variability in GPP obtained through the application of this method is consistent with the basic conceptual model of productivity that has emerged from decades of research on Chesapeake Bay. This consistency with previous work provides confirmation of the utility of the proposed method and highlights its potential for use in other less studied estuarine systems. Furthermore, this method provides spatially and temporally resolved estimates of GPP that can be used to more rigorously assess numerical biogeochemical models, which too often are not validated against the fundamental biological rates they are designed to simulate.

Acknowledgments
This paper is the result of research funded in part by NOAA's U.S. Integrated Ocean Observing System (IOOS) Program Office as a subcontract to the Woods Hole Oceanographic Institution under award NA13NOS120139 to the Southeastern University Research Association. All of the data analyzed in this paper are publicly available including the CBIBS data (http://buoybay.noaa.gov), the NCEP NARR data (https://www.esrl.noaa.gov/psd), and the Kd-490 MODIS data (ftp://ftp.star.nesdis.noaa.gov/pub/socd1/ecn/data/modis/k490noaa/monthly/cd/). Model output analyzed in this paper is publicly available through the THREDDS server associated with the IOOS Coastal and Ocean Modeling Testbed (COMT) site (https://comt.ioos.us/projects/cb_hypoxia). Postprocessed and compiled data for all seven CBIBS locations including the interpolated values of incoming solar radiation and satellite-derived Kd-490 can also be download from the COMT site.

References

Boynton, W. R., & Kemp, W. M. (1985). Nutrient regeneration and oxygen consumption by sediments along an estuarine salinity gradient. *Marine Ecology Progress Series*, *23*, 45–55.

Boynton, W. R., Kemp, W. M., & Keefe, C. W. (1982). A comparative analysis of nutrients and other factors influencing estuarine phytoplankton production. In V. S. Kennedy (Ed.), *Estuarine Comparisons* (pp. 69–90). New York, NY: Academic Press.

Cloern, J. E. (2001). Our evolving conceptual model of the coastal eutrophication problem. *Marine Ecology Progress Series*, *210*, 223–253.

Fennel, K., Wilkin, J., Levin, J., Moisan, J., O'Reilly, J., & Haidvogel, D. (2006). Nitrogen cycling in the Middle Atlantic Bight: Results from a three-dimensional model and implications for the North Atlantic nitrogen budget. *Global Biogeochem. Cycles*, *20*, GB3007. https://doi.org/10.1029/2005GB002456

Fisher, T. R., Harding, L. W. Jr., Stanley, D. W., & Ward, L. G. (1988). Phytoplankton, nutrients, and turbidity in the Chesapeake, Delaware, and Hudson estuaries. *Estuarine, Coastal and Shelf Science*, *27*(1), 61–93.

Fisher, T. R., Peele, E. R., Ammerman, J. W., & Harding, L. W. Jr. (1992). Nutrient limitation of phytoplankton in Chesapeake Bay. *Marine Ecology Progress Series*, *82*, 51–63.

Flemer, D. A. (1970). Primary production in the Chesapeake Bay. *Chesapeake Science*, *11*(2), 117–129.

Gallegos, C. L. (2012). Phytoplankton photosynthetic capacity in a shallow estuary: Environmental correlates and interannual variation. *Marine Ecology Progress Series*, *463*, 23–37.

Gallegos, C. L. (2014). Long-term variations in primary production in a eutrophic sub-estuary. *I. Seasonal and spatial patterns. Marine Ecology Progress Series*, *502*, 53–67.

Gallegos, C. L., & Neale, P. J. (2015). Long-term variations in primary production in a eutrophic sub-estuary: Contribution of short-term events. *Estuarine, Coastal and Shelf Science*, *162*, 22–34.

Harding, L. W. Jr. (1994). Long-term trends in the distribution of phytoplankton in Chesapeake Bay: Roles of light, nutrients and streamflow. *Marine Ecology Progress Series*, 267–291.

Harding, L. W. Jr., Meeson, B. W., & Fisher, T. R. Jr. (1986). Phytoplankton production in two east coast estuaries: Photosynthesis-light functions and patterns of carbon assimilation in Chesapeake and Delaware Bays. *Estuarine, Coastal and Shelf Science*, *23*(6), 773–806.

Howarth, R. W., Marino, R., Garritt, R., & Sherman, D. (1992). Ecosystem respiration and organic carbon processing in a large, tidally influenced river: The Hudson River. *Biogeochemistry*, *16*(2), 83–102.

Irby, I. D., Friedrichs, M. A., Friedrichs, C. T., Bever, A., Hood, R. R., Lanerolle, L. W., et al. (2016). Challenges associated with modeling low-oxygen waters in Chesapeake Bay: A multiple model comparison. *Biogeosciences*, *13*(7), 2011–2028.

Laws, E. A. (1991). Photosynthetic quotients, new production and net community production in the open ocean. *Deep Sea Research Part A. Oceanographic Research Papers*, *38*(1), 143–167.

Lomas, M. W., Glibert, P. M., Shiah, F. K., & Smith, E. M. (2002). Microbial processes and temperature in Chesapeake Bay: Current relationships and potential impacts of regional warming. *Global Change Biology*, *8*(1), 51–70.

Malone, T. C. (1992). Effects of water column processes on dissolved oxygen, nutrients, phytoplankton and zooplankton. In D. E. Smith, M. Leffler, & G. Mackiernan (Eds.), *Oxygen dynamics in the Chesapeake Bay. A synthesis of recent research*, (pp. 61–112). College Park, MD: Maryland Sea Grant.

Malone, T. C., Crocker, L. H., Pike, S. E., & Wendler, B. W. (1988). Influences of river flow on the dynamics of phytoplankton production in a partially stratified estuary. *Marine Ecology Progress Series*, *48*, 235–249.

Odum, H. T. (1956). Primary production in flowing waters. *Limnology and Oceanography*, *1*(2), 102–117.

Palinkas, C. M., Halka, J. P., Li, M., Sanford, L. P., & Cheng, P. (2014). Sediment deposition from tropical storms in the upper Chesapeake Bay: Field observations and model simulations. *Continental Shelf Research*, *86*, 6–16.

Pennock, J. R., & Sharp, J. H. (1986). Phytoplankton production in the Delaware Estuary: Temporal and spatial variability. *Marine Ecology Progress Series*, *34*, 143–155.

Sanford, L. P., Suttles, S. E., & Halka, J. P. (2001). Reconsidering the physics of the Chesapeake Bay estuarine turbidity maximum. *Estuaries*, *24*(5), 655–669.

Schubel, J. R. (1968). Turbidity maximum of the northern Chesapeake Bay. *Science*, *161*(3845), 1013–1015.

Scully, M. E. (2013). Physical controls on hypoxia in Chesapeake Bay: A numerical modeling study. *Journal of Geophysical Research: Oceans*, *118*, 1239–1256. https://doi.org/10.1002/jgrc.20138

Scully, M. E. (2016). The Contribution of physical processes to inter-annual variations of hypoxia in Chesapeake Bay: A 30-year modeling study. *Limnology and Oceanography*. https://doi.org/10.1002/lno.10372

Scully, M. E. (2018). A diel method of estimating gross primary production. Part 1: Validation with a realistic numerical model. *Journal of Geophysical Research: Oceans*, *123*. https://doi.org/10.1029/2018JC014178

Swaney, D. P., Howarth, R. W., & Butler, T. J. (1999). A novel approach for estimating ecosystem production and respiration in estuaries: Application to the oligohaline and mesohaline Hudson River. *Limnology and Oceanography*, *44*(6), 1509–1521.

Wang, M., Son, S., & Harding, L. W. (2009). Retrieval of diffuse attenuation coefficient in the Chesapeake Bay and turbid ocean regions for satellite ocean color applications. *Journal of Geophysical Research*, *114*, C10011. https://doi.org/10.1029/2009JC005286